

Evaluation Study on Corrosion Inhibitor and Tube/Rod Material Compatibility in CO₂ Injection-Production Wells

Huifang Song^{1,2}, Jingjing Qi¹, Kai Jin¹, Wei Huang¹, Yingbiao Xu¹,
Tingyi Wang¹

¹Shengli Oilfield Technology Testing Center, Dongying, Shandong, China

²Postdoctoral Research Station, Shengli Oilfield, Dongying, Shandong, China

Abstract. This paper evaluates the corrosion resistance performance of different corrosion inhibitors and tube/rod materials in the injection-production well environment of Carbon Capture, Utilization and Storage (CCUS) projects. Through laboratory corrosion tests, the inhibition effects of various corrosion inhibitors and their adaptability under different working conditions were analyzed. Results show that under extreme corrosive environments, conventional corrosion inhibitors have deficiencies in protecting standard tube/rod materials. The corrosion rates of conventional tube/rod materials are generally high and comparable. As temperature and CO₂ content (partial pressure) increase, there is a trend of increasing corrosion rates. Different materials show significant variations in corrosion resistance performance in CO₂-containing media. This paper provides scientific basis for the selection of corrosion inhibitors and tubing materials in CCUS projects.

Keywords: CCUS; Corrosion inhibitor; Tube/rod material; Corrosion resistance.

1. Introduction

Carbon Capture, Utilization and Storage (CCUS) technology is one of the important means to mitigate global climate warming[1]. In CCUS projects, injection-production well tubulars face serious corrosion problems due to contact with high concentrations of CO₂ and water[2-3]. Selecting appropriate corrosion inhibitors and corrosion-resistant materials is crucial for extending equipment life and ensuring engineering safety. This study evaluates the corrosion resistance performance of several common corrosion inhibitors and tube/rod materials in CO₂ environments through laboratory simulation experiments.

2. Experimental Materials and Methods

2.1. Experimental Instruments and Materials

The main reagents used in the experiments are shown in Table 1.

Table 1. Experimental Materials

| Classification | Main Reagents | Specifications |
|-------------------------------------|--------------------------|------------------|
| Formation water simulation reagents | NaCl | Analytical grade |
| | MgCl ₂ , etc. | Analytical grade |
| Corrosion coupon treatment reagents | Deionized water | Analytical grade |
| | Anhydrous ethanol | Analytical grade |

The equipment and instruments used in the experiments are shown in Table 2.

Table 2. Experimental Equipment

| Equipment Name | Manufacturer |
|--|--------------------------------|
| High-temperature high-pressure reactor | Shenggong Mechanical Co., Ltd. |
| Direct-reading spectrometer | Bruker Germany |
| Metallographic microscope | Zeiss Optical Company |

2.2. Experimental Methods

The experimental process followed the China Petroleum and Natural Gas Industry Standard SY 5405-1996. Before the experiment, test pieces were cleaned with anhydrous ethanol, dried with cold air, wrapped in filter paper, and stored in a desiccator[4-5]. Weight measurements were taken using an MS204S precision electronic balance before starting the experiment. Corrosion tests were conducted in high-temperature high-pressure reactors according to GB/T 4334.3-2000. The experimental setup is shown in Fig.1. For each experiment, three parallel samples were suspended and completely immersed in the corrosive medium, purged with nitrogen for 1h, heated to a specific temperature, and then pressurized with CO₂.

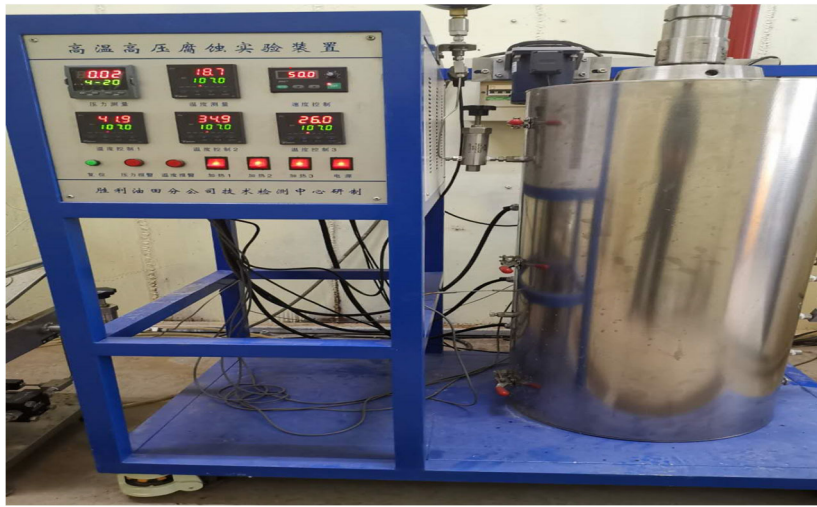


Figure 1. High-temperature high-pressure reactor

The corrosion rate and inhibition efficiency were calculated using equations 1 and 2:

$$\text{Corrosion rate: } V = \frac{8.76 \times 10^4 \times \Delta W}{S \times t \times \rho} \quad (1)$$

$$\text{Inhibition efficiency: } \eta = \left(\frac{V_0 - V}{V_0} \right) \times 100\% \quad (2)$$

Where, V_0 , V are corrosion rates without and with inhibitor respectively, in mm/a; S is sample surface area in cm²; t is test duration in h; ΔW is average weight loss in g; ρ is sample density in g/cm³.

2.3. Corrosion Inhibition Effect Evaluation

This study selected industrial corrosion inhibitors from five manufacturers and evaluated their corrosion inhibition effects under different dosages, temperatures, and CO₂ partial pressures by measuring corrosion rates and inhibition efficiencies. The specific experimental steps were:

a. Sample preparation: Common oil tube/sucker rod alloy steels N80, P110, and 30CrMo were selected as experimental materials, mechanically polished and chemically cleaned.

b. Solution preparation: Solutions with different inhibitor concentrations were prepared at 100mg/L, 500mg/L, 1000mg/L, and 1500mg/L.

c. Experimental setup: High-pressure reactors simulated actual downhole conditions with different temperatures and pressures, as shown in Table 3.

Table 3. Experimental Design and Conditions

| Dosage (mg/L) | CO ₂ Partial Pressure | | |
|--|----------------------------------|-------|-------|
| | 5MPa | 10MPa | 15MPa |
| 2000m (90°C, 20MPa) | 100, 500, 1000 | 1500 | 1500 |
| 3000m (130°C, 30MPa) | 100, 500, 1000 | 1500 | 1500 |
| Well Depth (Temperature, Total Pressure) | 100, 500, 1000 | 1500 | 1500 |

d. Data measurement: Corrosion rates were determined by weight loss method, and inhibition efficiencies were calculated.

2.4. Material Corrosion Resistance Testing Methods

Different grades of oil tubes and sucker rods were selected for corrosion experiments, focusing on corrosion rates in high-temperature ranges (60°C-130°C). Their corrosion resistance performance was evaluated in environments with different CO₂ contents. The experiments included metallographic analysis and corrosion rate determination under constant temperature and pressure. Specific steps were:

a. Material preparation: N80, P110, 30CrMo, Cr5, Cr9, Cr10, 1Cr13NiMo, 1Cr13 materials were selected and standard samples were prepared.

b. Experimental conditions: Corrosion rates were simulated under different well depth conditions, i.e., different CO₂ partial pressures and temperatures, for fixed durations (3, 6, 9, 12 days), as shown in Table 4.

Table 4. Experimental Conditions For Different Well Depths

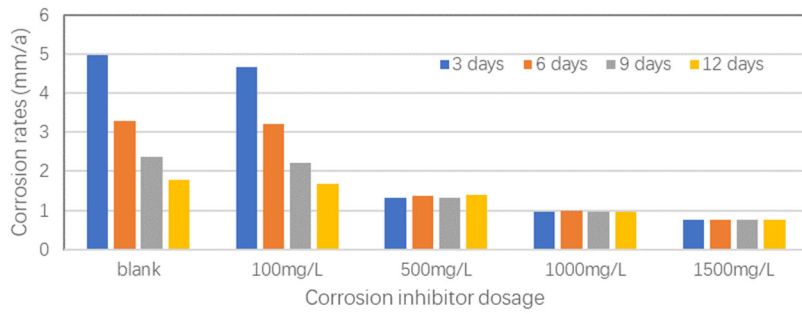
| Well Depth (Temperature, Total Pressure) | CO ₂ Partial Pressure/Content |
|--|--|
| 1000m (60°C, 10MPa) | 50%, 100%, / |
| 2000m (90°C, 20MPa) | 25%, 50%, 75% |
| 3000m (130°C, 30MPa) | 16.7%, 33.3%, 50% |

3. Results and Analysis

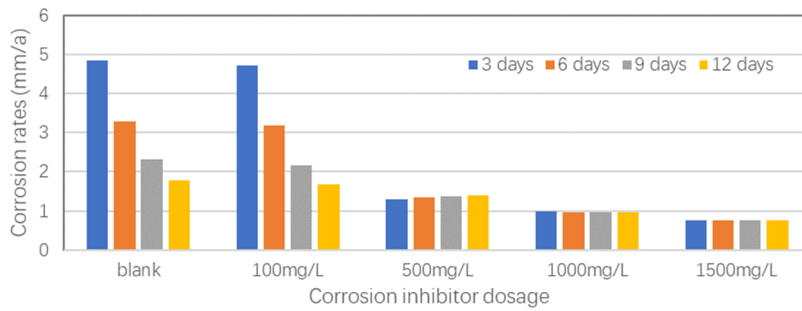
3.1. Evaluation of Corrosion Inhibitors

(1) Effect of Different Concentrations on Corrosion Rate at 3000m Well Depth

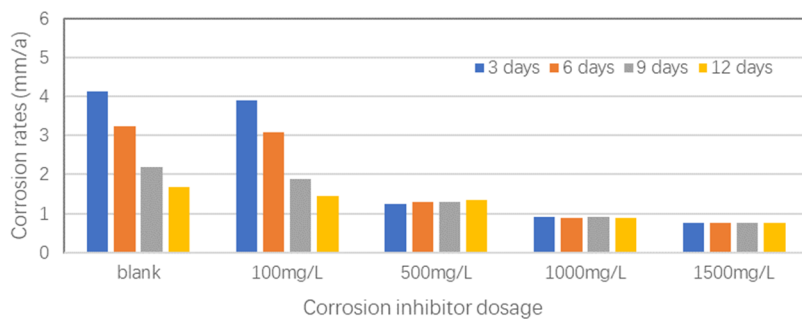
Fig.2 shows the corrosion rates of three common tube/rod materials with commercial corrosion inhibitor A at different dosages (100mg/L, 500mg/L, 1000mg/L, 1500mg/L) under 3000m well depth conditions. The results show that blank sample corrosion rates decreased over time, mainly due to the formation of corrosion products (such as oxides, hydroxides, etc.) on the sample surface. This corrosion product layer partially blocks contact between the metal and corrosive medium, thus reducing corrosion rate. At 100mg/L concentration, the corrosion rate was comparable to the blank group, indicating minimal effect at this well depth. At 500mg/L, corrosion rates remained stable within 12 days, showing some inhibition effect with efficiency around 60% and corrosion rates around 1.3mm/a for all three materials. At 1000mg/L, corrosion rates decreased to around 0.97mm/a with inhibition efficiency rising to 70%. At 1500mg/L, inhibition efficiency increased to around 77% with corrosion rates around 0.77mm/a.



(a) N80



(b) P110



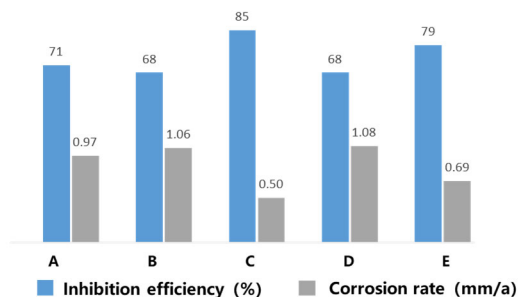
(c) 30CrMo

Figure 2. Corrosion rates with different corrosion inhibitor dosages at 3000m in-situ condition

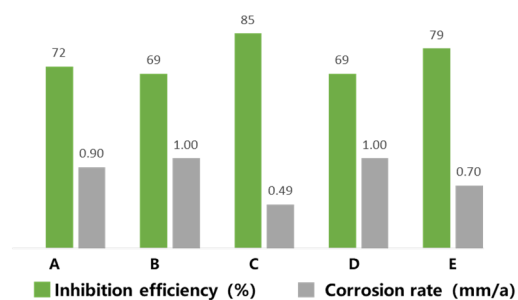
Corrosion inhibitors can be classified into various types based on their chemical structure and mechanism of action, including imidazoline derivatives, quaternary ammonium salts, organic amines, and surfactants. Imidazoline-type inhibitors mainly consist of imidazoline and its derivatives. Imidazoline is an organic compound containing a five-membered heterocycle, modified through substitution on the imidazoline nucleus to synthesize various derivatives. Imidazoline derivatives are weakly basic compounds that form hydrophobic, compact protective films on metal surfaces, preventing corrosive media (such as CO₂, H₂S) from contacting the metal substrate, thus providing corrosion inhibition. Due to their excellent inhibition effect and good environmental adaptability, they have become the most widely used type of corrosion inhibitor in oil and gas field CO₂ corrosion protection. Quaternary ammonium salt inhibitors are commonly used in oilfield water injection systems due to their excellent bactericidal and corrosion inhibition properties. They form stable protective films through electrochemical adsorption on metal surfaces, thus inhibiting CO₂ corrosion. Organic amine inhibitors prevent corrosion by forming hydrophobic films that prevent corrosive media from contacting metal surfaces. Surfactant-type inhibitors work by reducing surface tension on metal surfaces, forming uniform protective films to inhibit corrosion.

Currently, industrial corrosion inhibitors are mostly formulated using synergistic effects[6-7], and multi-component formulations are kept confidential. Fig.3 compares corrosion rates and inhibition efficiencies of different manufacturers' products at 1000mg/L and 1500mg/L dosages, shown with

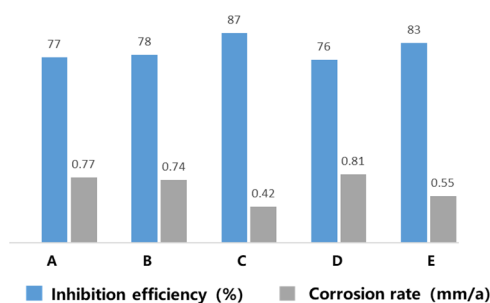
codes due to confidentiality requirements. Different manufacturers' inhibitors show varying effectiveness, with the best achieving over 80% inhibition efficiency. These differences mainly result from combined effects of chemical composition, physical form, manufacturing process, and additive components.



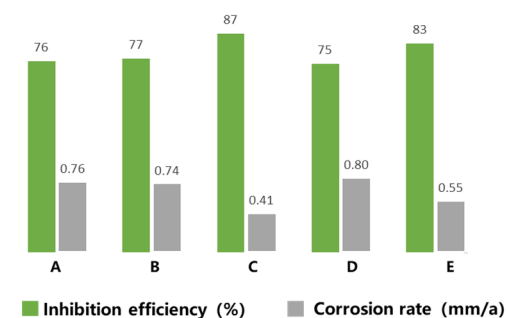
(a)



(b)



(c)

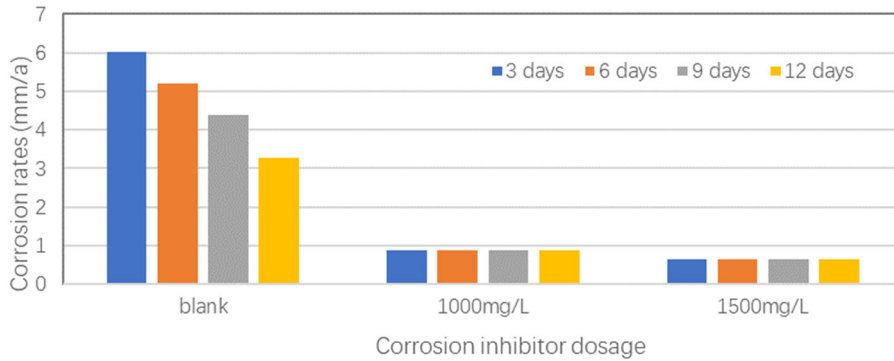


(d)

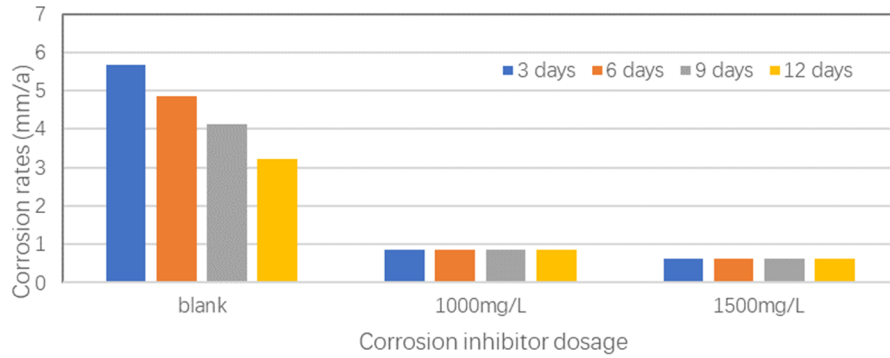
Figure 3. Inhibition efficiency comparisons: (a) Corrosion Inhibition Efficiency of Different Inhibitors on N80 Steel at 1000 mg/L, (b) Corrosion Inhibition Efficiency of Different Inhibitors on 30CrMo Steel at 1000 mg/L, (c) Corrosion Inhibition Efficiency of Different Inhibitors on N80 Steel at 1500 mg/L, (d) Corrosion Inhibition Efficiency of Different Inhibitors on 30CrMo Steel at 1500 mg/L.

(2) Effect of Different Concentrations on Corrosion Rate at 2000m Well Depth

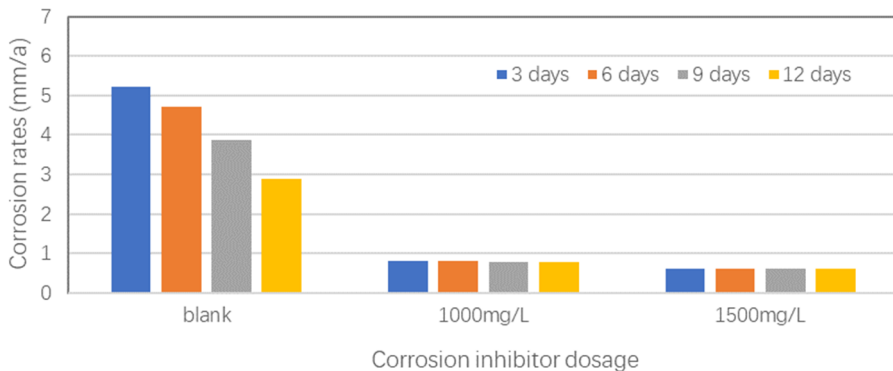
Fig. 4 shows the corrosion rates of three common tube/rod materials with commercial corrosion inhibitor A at different dosages (1000mg/L, 1500mg/L) under 2000m well depth conditions. Results indicate that at 1000mg/L dosage, the average inhibition efficiency reached 81% with corrosion rates $>0.85\text{mm/a}$. At 1500mg/L dosage, the average inhibition efficiency reached 86% with corrosion rates $>0.6\text{mm/a}$.



(a)N80



(b)P110



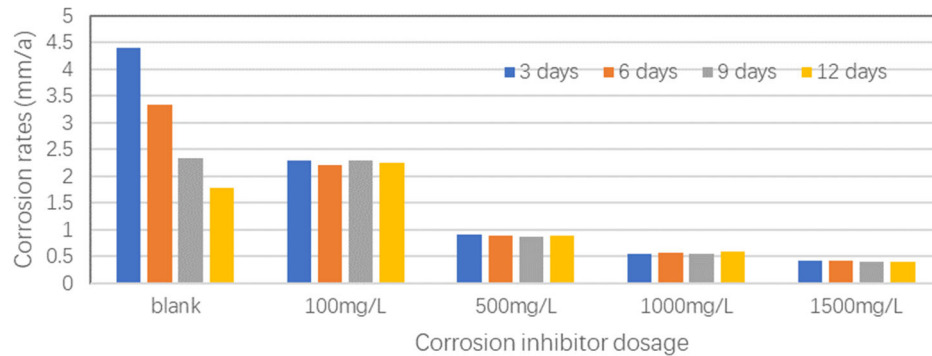
(c)30CrMo

Figure 4. Corrosion rates for N80, P110, and 30CrMo at 2000m in-situ condition

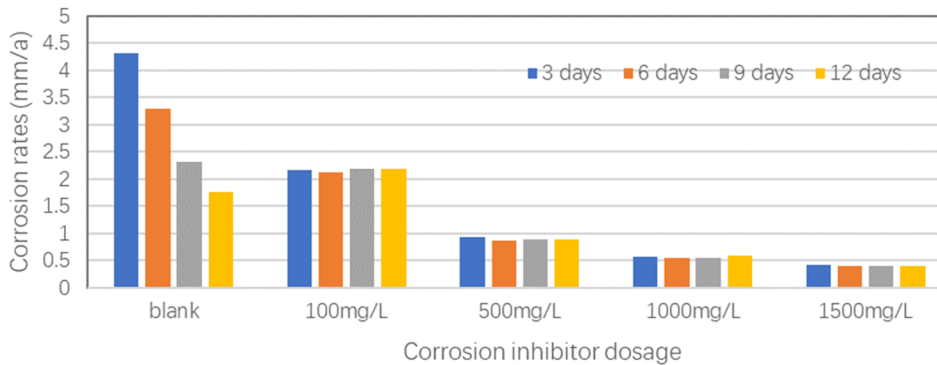
(3) Effect of Different Concentrations on Corrosion Rate at 1000m Well Depth

Fig. 5 shows the corrosion rates of three common tube/rod materials with commercial corrosion inhibitor A at different dosages (100mg/L, 500mg/L, 1000mg/L, 1500mg/L) under 1000m well depth conditions. At 100mg/L dosage, while there was some inhibition effect after adding the inhibitor, corrosion rates remained $>2.0\text{mm/a}$, indicating poor inhibition performance. At 500mg/L, inhibition efficiency improved but remained below 80%, with corrosion rates $>0.85\text{mm/a}$. At 1000mg/L,

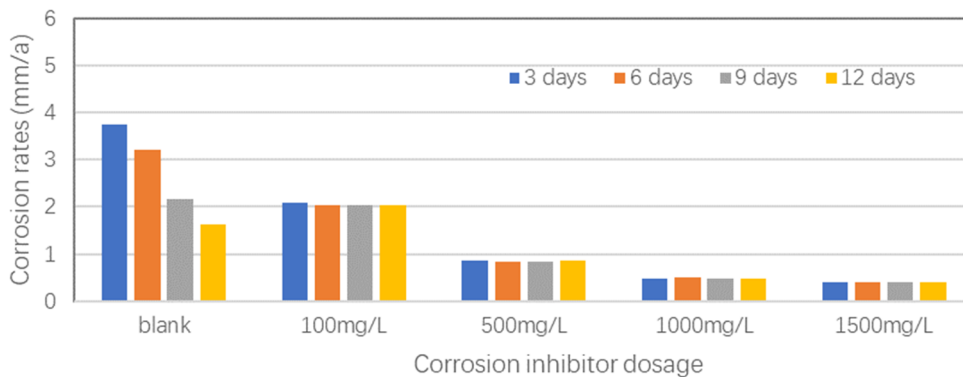
average inhibition efficiency reached 84% with corrosion rates $>0.5\text{mm/a}$. At 1500mg/L , average inhibition efficiency reached 87% with corrosion rates $>0.4\text{mm/a}$.



(a)N80



(b)P110



(c)30CrMo

Figure 5. Corrosion rates for N80, P110, and 30CrMo at 1000m in-situ condition

Fig. 6 compares inhibition efficiencies of different manufacturers' inhibitors under the same CO_2 partial pressure and dosage (CO_2 partial pressure 5MPa , dosage 1000mg/L) at different temperatures. Results show that various inhibitors maintain stable performance in the 60°C - 90°C range, but efficiency decreases by about 10% when temperature rises to 130°C . Comparing N80 material corrosion rate test results reveals that under extreme corrosive conditions (CO_2 partial pressure 5MPa , dosage 1000mg/L , mineralization 40000mg/L), none of the manufacturers' inhibitors could reduce conventional tube/rod material corrosion rates below 0.125mm/a , as shown in Fig. 7.

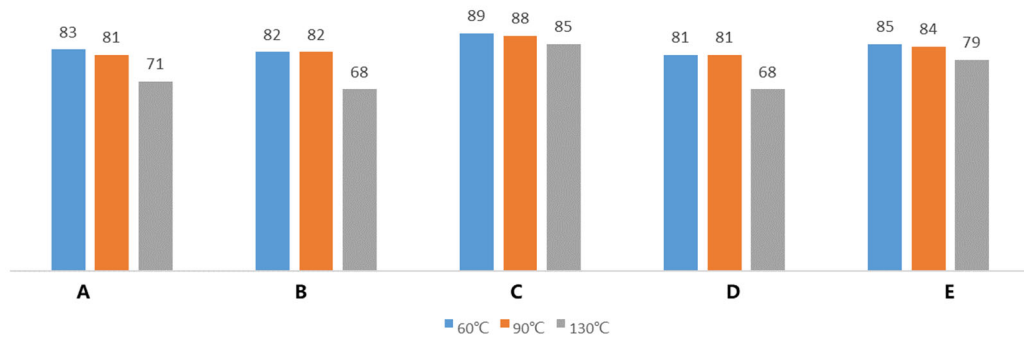


Figure 6. Temperature Effects on Corrosion Inhibition Efficiency of Different Manufacturers' Inhibitors Under the Same CO₂ Partial Pressure and Dosage Concentration

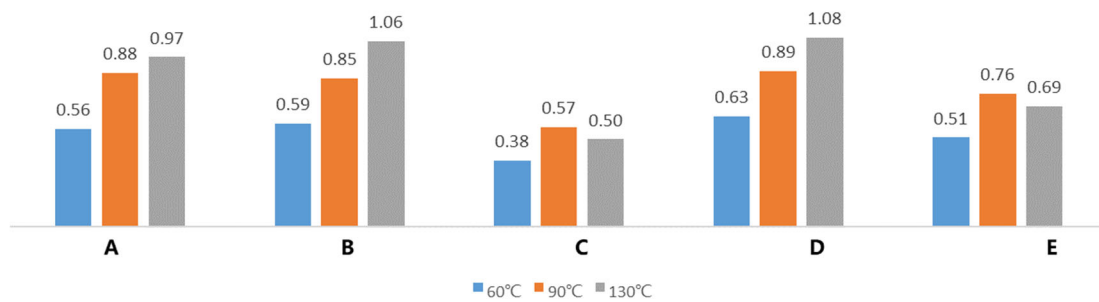


Figure 7. Temperature Effects on Corrosion Rate of N80 Steel Under the Same CO₂ Partial Pressure and Inhibitor Concentration

3.2. Corrosion Resistance Performance of Tube/Rod Materials

Different grades of oil tubes and sucker rods show distinct differences in corrosion resistance performance in CO₂ environments. Carbon steel corrosion rates increase significantly under high CO₂ partial pressure, while stainless steel and nickel-based alloys demonstrate excellent corrosion resistance[8-10]. Under high temperature and pressure conditions, stainless steel corrosion rates are significantly lower than carbon steel, with nickel-based alloys showing the lowest corrosion rates at only 1/5 that of carbon steel. This study selected multiple metal materials for corrosion resistance evaluation.

(1) Metallographic Structure

The microscopic structure of metallic materials directly determines their macroscopic mechanical properties. Fig. 8 shows microscopic structure analysis of different steel grades, clearly revealing the relationship between microstructural features (phase composition, grain size, and secondary phase distribution) and basic material properties. N80 steel's structure primarily consists of fine ferrite and small amounts of carbides. Normalized banded structure can be observed, closely related to N80 steel's heat treatment process. P110 has fine ferrite as the matrix with distributed pearlite particles, achieving good strength-toughness balance. For high-chromium steels like Cr5, Cr9, and Cr10, as chromium content increases, the metallographic structure transitions from ferrite-martensite to martensite-austenite, greatly improving material hardness, strength, and wear resistance. Additionally, Cr in stainless steel can react with O₂ to form stable Cr₂O₃ protective films, providing excellent corrosion resistance.

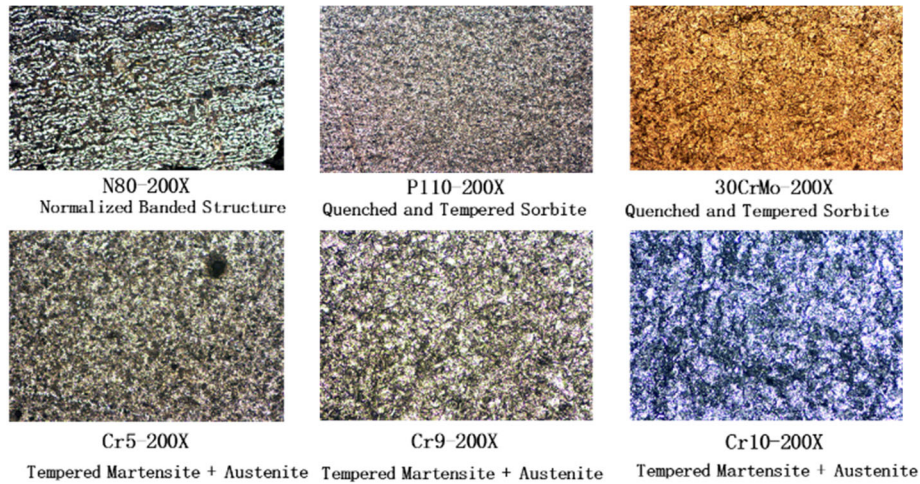
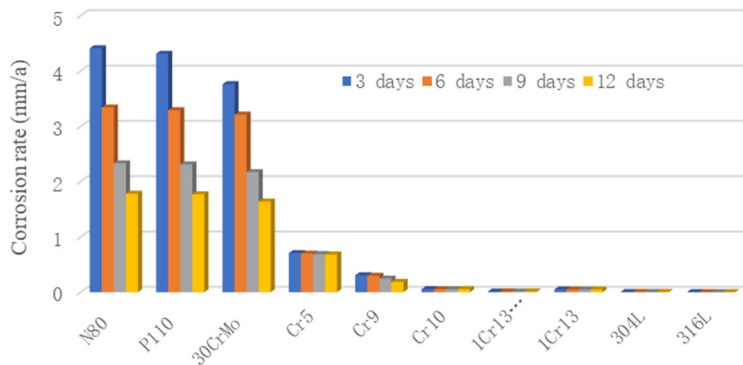


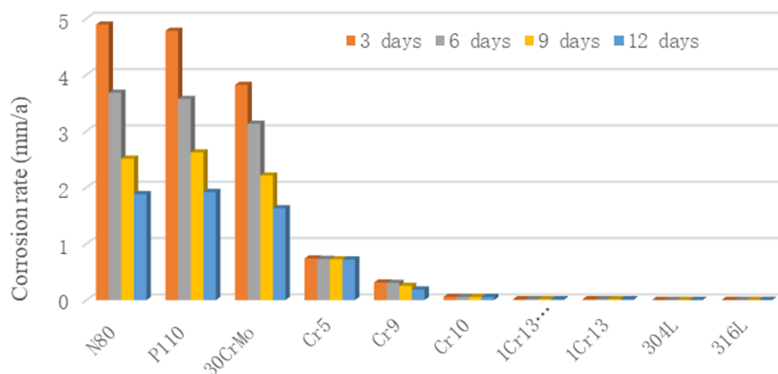
Figure 8. Metallographic analysis of different steel

(2) Tubing Material Corrosion Performance Evaluation

Fig. 9 shows corrosion rates of different tube/rod materials under different CO₂ partial pressures at 1000m well depth conditions. Under test conditions, conventional tube/rod materials show high initial corrosion rates that decrease over time. Due to stable experimental conditions, oxide films form on metal surfaces, while under dynamic conditions oxide films cannot form. New anti-corrosion materials maintain stable corrosion rates. CO₂ concentration significantly affects corrosion rates - compared to 5MPa CO₂ partial pressure, corrosion rates increase by about 10% at 10MPa CO₂ partial pressure, but impact on anti-corrosion materials is minimal. Cr10, 1Cr13NiMo, 1Cr13, 304L, and 316L materials show excellent corrosion resistance, all below the technical requirement of 0.125mm/a.



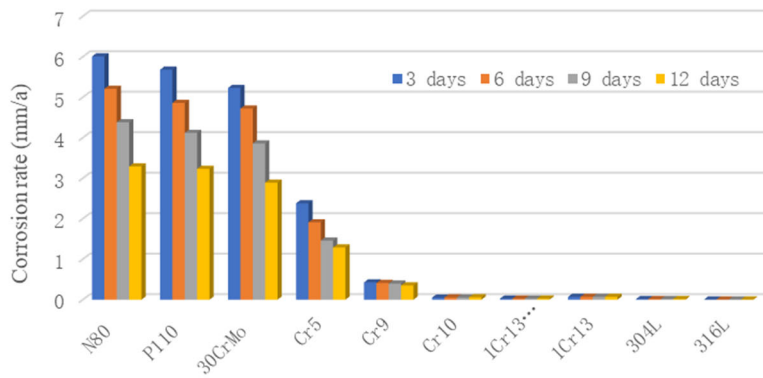
(a) CO₂ concentration 50%, 5MPa partial pressure



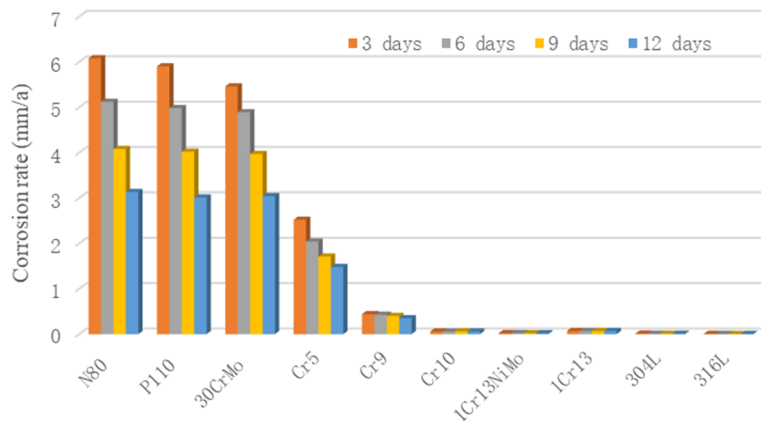
(b) CO₂ concentration 100%, 10MPa partial pressure

Figure 9. Corrosion rates under different CO₂ partial pressure at 1000m in-situ condition

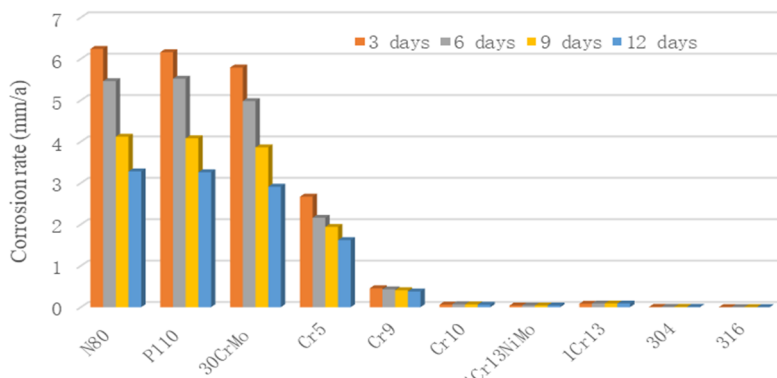
Fig. 10 shows corrosion rates of different tube/rod materials under different CO₂ partial pressures at 2000m well depth conditions. At 90°C, conventional materials' corrosion rates increase with CO₂ partial pressure while new materials remain largely unchanged, though all materials show varying degrees of increased corrosion rates compared to 60°C. However, materials like Cr10 and 316L maintain corrosion rates below 0.125mm/a, demonstrating excellent corrosion resistance.



(a) CO₂ concentration 25%, 5MPa partial pressure



(b) CO₂ concentration 50%, 10MPa partial pressure

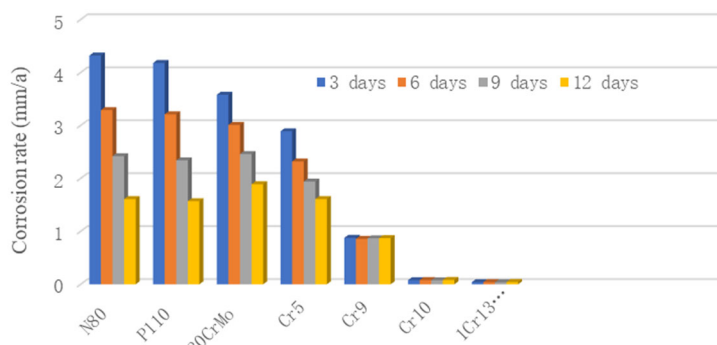


(c) CO₂ concentration 75%, 15MPa partial pressure

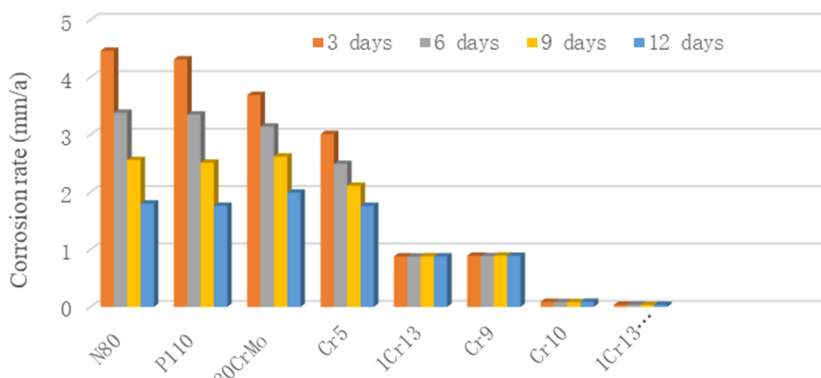
Figure 10. Corrosion rates under different CO₂ partial pressure at 2000m in-situ condition

Fig. 11 shows corrosion rates of different tube/rod materials under different CO₂ partial pressures at 3000m well depth conditions. At 130°C, conventional materials' corrosion rates increase with CO₂ partial pressure while new materials remain stable. Compared to 90°C, conventional carbon steel

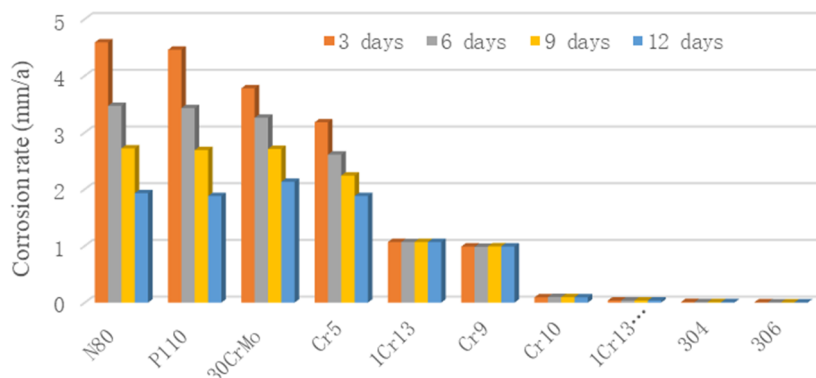
materials show slightly decreased corrosion rates at 130°C, while anti-corrosion tubing materials show slight increases.



(a) CO₂ concentration 16.7%, 5MPa partial pressure



(b) CO₂ concentration 33.3%, 10MPa partial pressure



(c) CO₂ concentration 50%, 15MPa partial pressure

Figure 11. Corrosion rates under different CO₂ partial pressure at 3000m in-situ conditon

4. Conclusions

Through laboratory simulation experiments, this study systematically evaluated the corrosion resistance performance of several corrosion inhibitors and tube/rod materials in CO₂ corrosive environments. The experimental results show:

A. The tested imidazoline-type composite corrosion inhibitors demonstrated excellent inhibition effects under various CO₂ partial pressures and temperature conditions, suitable for corrosion protection in CCUS injection-production wells. However, under extreme corrosive conditions (CO₂ partial pressure 5MPa, dosage 1000mg/L, mineralization 40000mg/L), none of the tested manufacturers' inhibitors could reduce conventional tube/rod material corrosion rates below 0.125mm/a.

B. Conventional tube/rod materials generally show high and comparable corrosion rates. Corrosion rates tend to increase with temperature and CO₂ content (partial pressure). Conventional tubing/rod materials, 5Cr, 9Cr, and conventional 13Cr cannot meet CCUS application conditions; anti-corrosion materials 1Cr13MoNi, 304L, and 316L achieve corrosion rates ≤ 0.076 mm/a; Cr10 material meets requirements of ≤ 0.076 mm/a at 90°C and ≤ 0.125 mm/a at 130°C, with Cr10 offering the best cost-performance ratio.

Through comprehensive evaluation of corrosion inhibitors and tube/rod materials, this study provides scientific basis for selecting corrosion inhibitors and tubing materials in CCUS projects, helping to improve equipment service life and engineering safety.

References

- [1] Bai YW, Kang YL, Chen LL. Analysis of Corrosion Characteristics of N80 CO₂ Injection String [J]. *Petrochemical Technology*, 2024, 31(05): 195-196.
- [2] Liu HW, Song XL, Ren L. Research on Corrosion Prevention Technology for CCUS-EOR Injection and Production Wells [J]. *Modern Occupational Safety*, 2024, (04): 37-43.
- [3] Cao YP, Lin WW, Feng JJ, et al. Prediction of Corrosion Rate in CO₂ Injection Well Tubing [J]. *Total Corrosion Control*, 2024, 38(02): 75-80.
- [4] Yu SC, Hu GX, Liu XC, et al. Current Status and Technical Research Direction of CO₂ Flooding Injection and Production Technology in Changqing Oilfield [J]. *Petrochemical Applications*, 2023, 42(12): 15-19.
- [5] Lu Y. Research on Mechanism and Structure-Activity Relationship of Modified Imidazoline Inhibitor in CO₂/H₂S Environment [D]. Beijing University of Chemical Technology, 2020.
- [6] Ouyang JL, Wang XX, Han X, et al. Study on Inhibition Effect of Imidazoline on CO₂ Corrosion in Oil-Water Alternating Environment [J]. *Journal of Chinese Society for Corrosion and Protection*, 2024, 44(03): 707-715.
- [7] Bai YZ, Su BY, Zhu XY, et al. Research Progress on Corrosion Mechanism of H₂S/CO₂ and Corrosion Inhibition System [J]. *Chemical Technology and Development*, 2024, 53(03): 36-40.
- [8] Qiuyu W, Wei W, Qing L, et al. Under-deposit corrosion of tubing served for injection and production wells of CO₂ flooding [J]. *Engineering Failure Analysis*, 2021, 127.
- [9] Wang Z, Cui R, Ma W, et al. Experimental Study on CO₂ Corrosion of Super 13Cr Integrated Tubing with Erosion Damage [J]. *Journal of Failure Analysis and Prevention*, 2019, 19(11): 1826-1831.
- [10] Farelas, F, Choi, et al. Corrosion Behavior of Deep Water Oil Production Tubing Material Under Supercritical CO₂ Environment: Part 2-Effect of Crude Oil and Flow [J]. *Corrosion*, 2014, 70(2): 137-145.